AAEC/E 115
TRG Report 532 (S/X)

UNCLASSIFIED

AAEC/E 115
TRG Report 532 (S/X)

AUSTRALIAN ATOMIC ENERGY COMMISSION

RESEARCH ESTABLISHMENT

LUCAS HEIGHTS

IRRADIATION OF BERYLLIUM AT ELEVATED TEMPERATURES

PART II

IRRADIATION OF RIG X–74 IN HIFAR

by

B. S. HICKMAN

G. BANNISTER

Issued Sydney, December 1963

UNCLASSIFIED

AUSTRALIAN ATOMIC ENERGY COMMISSION

RESEARCH ESTABLISHMENT

LUCAS HEIGHTS

IRRADIATION OF BERYLLIUM AT ELEVATED TEMPERATURES

PART II

IRRADIATION OF RIG X–74 IN HIFAR

by

B. S. HICKMAN

G. BANNISTER

ABSTRACT

Beryllium metal specimens fabricated by various routes were examined after irradiation to fast neutron doses of 5.5×10^{20} to 9×10^{20} nvt at temperatures of 450, 550, and 650 °C. The results were in general agreement with those reported previously for similar material irradiated to lower doses. Density changes of any significance were observed only at 650 °C. Serious loss of high temperature ductility occurred in all materials and was again attributed to helium bubble formation at grain boundaries. Material fabricated by hot pressing and extrusion showed superior properties, both before and after irradiation, to material prepared by loose sintering and extrusion.

The work described in this report was done under contract to the United Kingdom Atomic Energy Authority

CONTENTS

(continued)

CONTENTS (continued)

1. INTRODUCTION

As a part of the programme of studies carried out by the United Kingdom Atomic Energy Authority on the irradiation behaviour of canning materials for the fuel elements of the Advanced Gas Cooled Reactor (A.G.R.), beryllium metal has been irradiated at elevated temperatures in fast flux facilities in the Australian Atomic Energy Commission's reactor HIFAR. Two series of tests have been carried out. The results of the first test (Rig X–17) have already been reported (Hickman et al. 1963). The present report describes the second test in the series (Rig X–74) in which another series of samples was examined after a higher neutron dose. In general the experimental methods were the same for both tests and are described in detail in the earlier report. The programme has now been terminated and no further work is planned.

2. EXPERIMENTAL TECHNIQUES

2.1 Specimens

The specimens were fabricated by the Reactor Fuel Element Laboratories, U.K.A.E.A. Springfields.

The fabrication methods of the six groups of specimens identified by the codes B2.1 to B2.6 inclusive are listed in Table 1. Material B2.4 (loose sintered, warm extruded) is the same as material B1.2 in the X–17 test, but otherwise the fabrication methods were different from those used in the first test. It will be noted that materials B2.2, B2.3, and B2.6 were all fabricated by the same roure, that is hot pressing followed by hot and warm extrusion, but that material B2.3 was subjected to a slow cool annealing treatment after fabrication. Materials B2.1 and B2.4 differ only in the starting material. Materials B2.4 and B2.5 were fabricated by the same route from the same source material but the latter was subjected to the slow cool annealing treatment.

Three sets of specimens were supplied to be used as follows:

(1) One set for irradiation and subsequent testing, referred to as the irradiation specimens.

(2) One set to be tested as machined, referred to as the as–received specimens.

(3) One set to be tested after receiving the same thermal treatment as was received by the irradiated specimens, referred to as the heat-treated specimens.

2.2 Pre–Irradiation Measurements

The dimensions of all specimens were measured using a precision micrometer. The densities of the swelling specimens were measured by a displacement technique using n–octyl alcohol as the gravimetric fluid.

2.3 Irradiation Rig

The irradiation rig was described in detail in the previous report. The specimens were supported by ceramic spacers in six graphite carriers. Each graphite carrier contained a furnace element which was used to maintain the specimen temperature at the desired value. The stringer of six carriers was suspended from a shield plug inside the stainless steel thimble which could be purged with pure helium and then sealed.

2.4 Post–Irradiation Examination Procedure

Post–irradiation examination was carried out as follows:

(i) Visual examination – all specimens.

(ii) Dimensions – all specimens.

(iii) Density – all swelling specimens.

(iv) Tensile testing – all tensile specimens.

(v) Macrophotography – fracture faces of all tensile specimens.

(vi) Optical metallography – gauge lengths of all tensile specimens of material B2.2 and B2.3.

(vii) Electron microscopy – selected specimens of material B2.2, B2.3, B2.4, and B2.5.

Density and dimensions were measured as described in Section 2.2. Mechanical testing was done at the irradiation or out–of–pile heat–treatment temperature (that is 450, 550, or 650°C) at a strain rate of 12 per cent./hour. The load–elongation curves were recorded on a x – y recorder, the elongation being obtained from the movement of the cross heads. The elongation at fracture (obtained by re–assembling the specimen after testing, and measuring the distance between the shoulders) was checked from the recorder chart. Figures for the 0.1% and 0.5% proof stress and U.T.S. were taken from the recorder chart. Reduction in area was measured with a micrometer on the fractured test specimen.

Metallographic examination was carried out after mounting, grinding, and polishing with alumina on vibratory machines. Electron microscopic examination was made on replicas prepared from specimen surfaces obtained by fracturing at room temperature.

Helium analyses were carried out by the vacuum fusion method. In this method the sample is melted and the evolved gases collected and analysed by gas chromatography techniques.

2.5 Out–of–Pile Controls

The out–of–pile control specimens (set 2) were supported in graphite carriers and canned in stainless steel in a pure helium atmosphere and were subjected to the same heat treatment as the irradiated specimens.

To avoid confusion the term annealing is used throughout this report to describe the slow cool anneal heat treatment which was received by some of the materials (B2.3 and B2.5) after machining, and the term heat treatment is used to describe the heat treatment which was received by one group of specimens as described above.

3. OPERATING CONDITIONS DURING IRRADIATION

3.1 Irradiation Position

The rig was loaded into the A.3 hollow fuel element position on 21st November 1960, was transferred to the B.3 hollow fuel position on 21st December 1960, and was finally unloaded on 20th November 1961. The integrated reactor power levels were 251 MWd for the A.3 position and 2341 MWd for the B.3 position.

3.2 Irradiation Temperatures

The temperature histories of the carriers in the rig are shown in Figure 1. To avoid any possible overheating of the shield plug the heater currents were limited initially to a 6 amp maximum. Because of this limitation the temperatures obtained in carriers C, D, E, and F were lower than the desired values of 550 and 650°C and the rig operated for the first period with carriers A and B at the desired value of 450°C but with the other carriers in the range 500 – 540°C. In order to increase these temperatures without increasing the heat input to the furnaces the rig was moved at the end of the first period from the A.3 position to the B.3 position, which is nearer the core. The higher gamma heating in this position resulted in carriers E and F reaching the desired temperature of 550°C but carriers C and D were still 20 – 75°C lower than the desired value of 650°C. At the end of the next period (programme 15) the restriction on heater

current was removed (after tests had shown that no overheating of the plug occurred) and the temperatures of all carriers were raised to the desired values, namely:

A	B	C	D	E	F
450°C	450°C	650°C	650°C	550°C	550°C .

This situation continued until the irradiation was 75 per cent. complete when heater C failed and the temperature of this carrier, which was then operating on gamma heating alone, fell and remained in the range 490 – 520°C for the rest of the irradiation. Towards the end of the irradiation the temperature of carrier B exceeded the control temperature of 450°C by up to 50°C with the furnace turned off. This was due to high gamma heating associated with higher reactor power levels and changes in rig loading.

For the rest of this report the irradiation temperatures referred to are the desired control temperatures listed above. Reference should be made to Figure 1 for the variations from these values.

3.3 Rig Atmosphere

The rig atmosphere was controlled by purging the rig at each shutdown with helium purified by molecular sieves (as described by Hickman et al. (1963)) until the moisture and oxygen levels detected in the outlet were less than 50 p.p.m. Often, however, the levels could not be reduced to below 100 p.p.m. The rig was then sealed off at a positive pressure of about 2 p.s.i. Gas samples taken at shut-downs showed that some in-leakage of air and water had occurred.

3.4 Reactor Power

The reactor power for most of the irradiation was between 9 and 11 MW (thermal).

4. RESULTS

4.1 Visual Examination

The specimens from carriers C, D, E, and F were oxidized, the oxidation being worse in carriers C and D. However, the oxidation appeared to be somewhat less than that observed in Rig X-17 specimens and this was subsequently confirmed by metallographic examination.

The specimens were successfully identified either by carrier position or inscribed markings which were generally still visible in spite of the oxidation.

4.2 Dose

On dismantling the rig in the remote handling facilities, the graphite carriers were found to be cracked and most of the cobalt monitors fell out. Hence their position could not be positively identified. Five of the six monitors were recovered and the thermal neutron doses calculated from these monitors are compared in Table 2 with the thermal and fast neutron doses calculated from the data obtained during low power operation of HIFAR and from other adjacent rigs. The fast neutron doses quoted are the integrated doses over the fission neutron spectrum. The doses above 1 MeV would be approximately 70 per cent. of these values.

4.3 Density and Dimensions

No significant dimensional or density changes were determined on any specimens after heat treatment at any temperature or after irradiation at 450°C. Owing to excessive oxidation the dimensional and density changes of the specimens irradiated at 550°C and 650°C had little meaning. The swelling specimens irradiated at these temperatures were etched in a chromic-sulphuric-phosphoric acid mixture to remove the oxide film and the densities were re-determined (see Table 3). Only a few specimens irradiated at 550°C showed changes outside the experimental error (± 0.1 per cent.). Irradiation at 650°C produced a significant decrease in density in all the specimens, the change being most marked in materials B2.1, B2.5, and B2.6.

4.4 Tensile Tests

The results of the tensile tests for the six materials are given in Tables 4 – 9 and the results are plotted in graphical form in Figures 2 – 9. All specimens were tested at their nominal irradiation or heat treatment temperature, that is 450, 550, and 650°C.

Comparison of the behaviour of the six different materials shows similar trends to those observed in the first series of tests. Heat treatment resulted in large changes in properties over the as-received condition. There was an increase in elongation and a decrease in proof stress and U.T.S. in almost all cases. Irradiation generally reversed this trend, that is there was a considerable increase in proof stress and U.T.S. over the values for the heat-treated specimens, and the proof stress generally was higher than for the as-received specimens while the U.T.S. was much the same. The ductility of the irradiated specimens was very low at 650°C, and in materials B2.1, B2.4, and B2.5 was still very low at 550°C

Comparison of the behaviour of material B2.4 with the nominally identical material B1.2 from the first series (Hickman et al. 1963) shows that the results for the as-received specimens were much the same for the two cases. After heat treatment the B2.4 series showed similar properties at 450 and 650°C to B2.1 but considerably smaller ductility at 550°C. After irradiation the U.T.S. and yield strength were generally higher and the elongation and reduction in area somewhat less for material B2.4 than for material B1.2. This behaviour was most marked at 450°C and is presumably a direct result of the higher dose to which the second series was irradiated.

Comparison of the behaviour of materials B2.2, B2.3, and B2.6, all of which were fabricated by the same route, namely hot pressed, hot extruded, and then warm extruded, shows that little significant difference in behaviour resulted from slow cool annealing treatment to which material B2.3 was subjected. The properties of the two materials were much the same in the as-received, heat-treated, and irradiated conditions.

In the as-received and irradiated condition there was little difference in the properties of the loose sintered and extruded materials (B2.1 and B2.4). The heat-treated specimens showed similar properties at 450°C and 650°C but the loose sintered material had a considerably higher ductility at 550°C. The annealed material (B2.5) showed greater ductility and lower proof stress in the as-received and heat-treated conditions than the non-annealed material (B2.4) but after irradiation the properties of all three loose sintered and extruded materials were very similar.

All the loose sintered and extruded materials showed lower strength and ductility than the hot pressed and extruded materials under similar conditions.

The examination of the fracture surfaces showed no evidence for cleavage failure under any conditions. Owing to the fine grain size of the material it was difficult to distinguish between intergranular and ductile shear failure but specimens tested at 650°C generally showed fairly obvious intergranular failure.

4.5 Metallographic Examination

Metallographic examination of the samples of each material irradiated at 650°C was carried out to determine the depth of oxidation. The depth of penetration of corrosion products varied from 5 – 50 μ in material B2.4 to 100 – 150 μ in material B2.2.

Materials B2.2 and B2.3 only were subjected to detailed metallographic examination and in general showed the same features as those observed in the X-17 specimens. Specimens tested at 450 and 550°C which showed large reduction in area exhibited evidence of deformation within the grains. The fracture was generally intergranular at 650°C and mainly transgranular at 450°C. At 550°C the heat treated specimens showed transgranular failure but in the irradiated specimens there was much intergranular failure. Transverse cracking apparently resulting from the link-up of voids was observed at all temperatures but, as for the previous tests, was most obvious in the specimens heat treated at 650°C and in these specimens extended for a considerable distance back from the fracture. Little difference in behaviour was observed between the two materials examined.

4.6 Electron Microscopic Examination

The results of electron microscope examination of materials B2.2, B2.3, B2.4, and B2.5 irradiated at 550°C and 650°C are summarised in Table 10.

Intergranular and intragranular bubble formation was observed in all these materials, more bubbles being observed at 650°C than at 550°C.

Comparison of the hot pressed and extruded materials B2.2 and B2.3 shows that intergranular bubble formation was greater and intragranular bubble formation somewhat less in the annealed material B2.3 than in the non-annealed material B2.2 (Figure 10). The intergranular bubble formation in the loose sintered material B2:4 was considerably greater than in the hot pressed and extruded materials but little bubble formation was evident on cleavage flakes in this material (Figure 11). The bubble formation in this material (B2.4) was somewhat greater than in the corresponding material B1.2 in rig X-17 as would be expected with the higher neutron dose.

4.7 Helium Analysis

The results of helium analysis on selected samples are shown in Table 11 together with quantities calculated using the neutron dosimetry data and effective fission spectrum cross sections of 100 mb and 25 mb for the (n,2n) and (n, α) reactions respectively. It can be seen that there is good agreement between the measured and calculated values except for carrier F where the measured values are about 20 per cent. lower than the calculated values.

5. DISCUSSION

The results described confirm the previous conclusions (Hickman et al. 1963; Hyam and Sumner 1962) that considerable loss of high temperature ductility can occur when beryllium is irradiated at elevated temperatures and that this is due to helium bubble formation at the grain boundaries. The bubbles are thought to act as nuclei for the stress-induced void formation which precedes fracture at these temperatures.

The factors which determine the distribution of helium bubbles in irradiated beryllium are as yet incompletely understood. Previous work at this laboratory (Hickman et al. 1963; Chute 1963) has shown that the distribution is very dependent on material history as well as dose and temperature. Analysis of the results from the first experiment in this series suggested that the nucleation of gas bubbles occurred at second phase precipitates and that variations in the distribution of these precipitates caused variations in the bubble distribution from material to material.

Whilst no direct evidence has as yet been obtained for this hypothesis recent results of electron microscopy studies, electrical resistivity changes, and mechanical property changes have been interpreted satisfactorily in terms of nucleation of bubbles at an iron-rich precipitate whose distribution is markedly affected by heat treatment (Hickman and Chute 1963). In material in which the heat treatment is such as to produce a very fine distribution of this phase, bubble nucleation occurs on a very fine scale within the grains with very little bubble formation at the grain boundaries. When this material is irradiated to doses similar to those received by the samples described in this report, no bubbles can be observed by replica electron microscopy for an irradiation temperature of 550°C, and at 600 - 700°C bubble formation is much less than that observed in the present experiments (Chute, 1963). On the other hand, material which has been heat treated to coarsen the iron-rich precipitate shows extensive grain boundary bubble formation similar to that observed in these experiments caused by lack of nuclei for bubble formation within the grains. This material then shows loss of high temperature ductility owing to the bubbles acting as nuclei for stress-induced void formation as discussed by Hyam and Sumner (1962).

At first glance the results described in this report do not altogether support this hypothesis. In particular very little difference in behaviour was noted between the hot pressed and extruded materials B2.2 and B2.3 although the latter was subjected to the slow cool anneal treatment which is designed to precipitate the iron in coarse form at the grain boundaries. However, examination

of the tensile properties of these two materials showed that the expected changes on annealing did not occur. This suggests either that the thermal treatment received by the as-fabricated material during fabrication produced the same impurity distribution as the slow cool anneal or that the slow cool anneal treatment was not effective in significantly changing the impurity distribution. In view of this it is not surprising that little difference in behaviour was observed.

The loose sintered and extruded materials also showed little difference in behaviour after irradiation although it was apparent from the tensile properties that the slow cool annealing treatment had affected tensile properties in the as-received condition. The similar bubble distribution observed by electron microscopy in the annealed material (B2.4) and the non-annealed material (B2.5) presumably results in the similar tensile properties observed in these materials after irradiation. The fact that considerable grain boundary bubble formation was observed at 550°C in the non-annealed material again suggests, as with the hot pressed and extruded materials, that the thermal history of these specimens was such as to remove nucleation sites from within the grains and that the subsequent slow cool anneal treatment produced no further significant change in the impurity distribution as it affects bubble nucleation.

It is not clear whether the inferior properties of the loose sintered and extruded materials after irradiation were due to their poorer initial properties or to the greater amount of grain boundary bubble formation observed in these materials. However, as mentioned above, these materials all showed similar properties after irradiation whereas the as-received and heat treated specimens showed different properties. Hence it would appear that bubble formation was the prime factor in determining their properties and their inferiority to the hot pressed and extruded materials.

6. CONCLUSIONS

1. The results confirm previous observations that a considerable reduction in high temperature ductility can occur where beryllium metal is irradiated at elevated temperatures and that this is due to helium bubble formation at grain boundaries.

2. Material fabricated by hot pressing and extrusion showed superior tensile properties to material fabricated by loose sintering and extrusion in both the as-received and irradiated conditions. The superiority in the irradiated condition was probably due to the smaller amount of grain boundary bubble formation in the former material.

3. The pre-irradiation slow cool annealing treatment did not result in any change in the properties of the hot pressed and extruded materials either before or after irradiation. This annealing treatment resulted in improved pre-irradiation properties of the loose sintered and extruded materials but no difference was observed in the properties after irradiation.

4. There were no significant differences in behaviour of loose sintered and extruded materials prepared from powder from two different commercial suppliers.

7. ACKNOWLEDGMENTS

The authors wish to acknowledge the help of the following in the work described in this report: The Rig Group for assembly and testing of the irradiation rig, Reactor Operations Section for supervision of the rig operation, Analytical Chemistry Section for analyses of the rig atmosphere and determination of helium in the irradiated samples, Hot Cells Group for rig disassembly and preliminary examination of the samples, J. McCracken for the metallography, and J. Chute for the electron microscopy.

8. REFERENCES

Chute, J. (1963). – AAEC/E108.

Hickman, B.S., Bell, J.C., Bannister, G., McCracken, J., Chute, J., and Smith, R. (1963). – TRG Report 540(S/X).

Hickman, B.S., and Chute, J. (1963). – J. Aust. Inst. Metals 8: 298.

Hyam, E.D., and Sumner, G. (1962). – Proc. of I.A.E.A. Conference on Radiation Damage in Solids, Venice. Vol. 1 p.323.

TABLE 1

DETAILS OF FABRICATION METHODS USED IN THE INVESTIGATION.

The slow cool annealing treatment involved soaking for 2 hours at 850°C and then cooling at 2½ deg/hour.

Code	Fabrication Method	Annealing Treatment
B 2.1	Loose sintered, warm extruded	None
B 2.2	Hot vacuum pressed, hot extruded, and then warm extruded	None
B 2.3	" " "	Slow cool anneal
B 2.4	Loose sintered, warm extruded	None
B 2.5	" " " "	Slow cool anneal
B 2.6	Hot vacuum pressed, hot extruded, and then warm extruded	None

TABLE 2

MEASURED AND CALCULATED NEUTRON DOSES

Carrier	Nominal Irradiation Temperature (°C)	Calculated Dose (nvt Thermal)	Measured Dose (nvt Thermal)	Calculated Dose (nvt Fast)
A	450	2.1×10^{21}	)	5.5×10^{20}
B	450	2.65×10^{21}	)	7.0×10^{20}
C	650	3.4×10^{21}	) $1.7 - 3.0 \times 10^{21}$	9.0×10^{20}
D	650	3.5×10^{21}	)	9.0×10^{20}
E	550	3.4×10^{21}	)	9.0×10^{20}
F	550	3.2×10^{21}	)	8.5×10^{20}

TABLE 3

DENSITY CHANGES MEASURED ON SPECIMENS AFTER IRRADIATION AT 550°C AND 650°C

The measurements were made after removal of the oxide corrosion products by etching.

Material	Density Change (per cent.)	
	550°C	650°C
B 2.1	< 0.1	– 1.2
B 2.2	< 0.1	–0.25
B 2.3	– 0.2	–0.4
B 2.4	– 0.25	– 0.4
B 2.5	– 0.1	– 1.1
B 2.6	– 0.25	– 1.5

TABLE 4

TENSILE RESULTS FROM MATERIAL B 2.1

Irradiation Temp. (°C)	Condition	Spec. No.	0.1% Proof Stress (p.s.i.)	U.T.S. (p.s.i.)	% Elong.	% R of A
450	Irradiated	1.1	22,000	22,900	2.7	5.9
		1.2	22,300	23,200	2.3	3.6
	Heat treated	1.7	12,500	14,000	25.5	30
		1.8	12,500	13,600	23.5	30
	As received	1.5	16,300	21,900	13.0	22
		1.6	16,100	20,200	9.6	12
500	Irradiated	1.9	11,700	11,800	2.3	2.5
		1.10	14,100	14,600	4.7	3.4
	Heat treated	1.15	7,900	8,430	26	28
		1.16	6,800	7,220	27	26
	As received	1.13	11,700	14,100	8.0	6.8
		1.14	10,800	12,850	8.8	7.5
650	Irradiated	1.17	4,800	4,800	2.6	1.1
		1.18	4,900	4,900	0.6	1.5
	Heat treated	1.23	5,200	5,400	11.5	8.8
		1.24	5,700	6,000	13.0	9.7
	As received	1.21	4,200	4,900	7.9	5.8
		1.22	4,500	5,000	8.5	5.8

TABLE 5

TENSILE RESULTS FROM MATERIAL B 2.2

Irradiation Temp. (°C)	Condition	Spec. No.	0.1% Proof Stress (p.s.i.)	U.T.S. (p.s.i.)	% Elong.	% R of A
450	Irradiated	2.1	31,700	31,800	16	34.5
		2.2	32,700	32,800	16	31
	Heat treated	2.7	21,000	26,000	32	53
		2.8	21,700	26,000	27	51
	As received	2.5	24,000	31,500	24	38
		2.6	23,900	33,300	21	38
550	Irradiated	2.9	16,900	18,000	6.3	6.1
		2.10	18,800	19,600	6.1	8.3
	Heat treated	2.15	14,300	16,500	24	29
		2.16	13,400	14,900	27	27
	As received	2.13	13,100	16,800	21	17
		2.14	14,700	17,800	24	21
650	Irradiated	2.17	7,200	7,900	3.9	5.2
		2.18	7,400	7,900	4.1	3.2
	Heat treated	2.23	3,900	5,400	22.5	17
		2.24	4,550	5,600	20	20
	As received	2.21	3,600	4,600	23	18
		2.22	4,500	5,000	24	17.5

TABLE 6

TENSILE RESULTS FROM MATERIAL B 2.3

Irradiation Temp. (°C)	Condition	Spec. No.	0.1% Proof Stress (p.s.i.)	U.T.S. (p.s.i.)	% Elong.	% R of A
450	Irradiated	3.1	31,100	31,200	23	37.5
		3.2	30,200	31,000	17	35
	Heat treated	3.7	19,200	24,700	28	54
		3.8	21,100	25,000	45	53
	As received	3.5	22,950	30,600	24	50
		3.6	26,000	30,200	23	49
550	Irradiated	3.9	17,700	18,700	9.1	7.1
		3.10	18,100	18,700	8.3	8.3
	Heat treated	3.15	14,100	15,300	27	25
		3.16	12,700	14,200	25	24
	As received	3.13	16,900	19,400	23	23
		3.14	15,900	19,200	22	19
650	Irradiated	3.17	7,300	8,100	5.4	1.9
		3.18	8,000	8,800	4.5	2.7
	Heat treated	3.23	3,900	6,000	16	9.9
		3.24	4,800	5,800	20	9.8
	As received	3.21	4,700	5,300	19	18
		3.22	4,800	5,600	19	14

TABLE 7

TENSILE RESULTS FROM MATERIAL B 2.4

Irradiation Temp. (°C)	Condition	Spec. No.	0.1% Proof Stress (p.s.i.)	U.T.S. (p.s.i.)	% Elong.	% R of A
450	Irradiated	4.1	24,100	27,300	23	45
		4.2	19,000	20,750	3.5	5.2
	Heat treated	4.7	11,900	13,300	30	35
		4.8	11,700	13,900	29	31.5
	As received	4.5	15,850	21,700	12	16.5
		4.6	16,550	22,400	14.5	19
550	Irradiated	4.9	11,400	11,700	1.2	3.3
		4.10	10,400	11,000	1.1	0.6
	Heat treated	4.15	6,300	6,740	13	18
		4.16	6,400	7,020	10.5	14
	As received	4.13	8,600	11,000	8.3	7.5
		4.14	8,500	10,300	8.8	6.1
650	Irradiated	4.17	–	3,100	0.9	1.2
		4.18	–	4,000	0.8	2.8
	Heat treated	4.23	3,900	4,500	8.0	7.5
		4.24	4,000	4,300	9.1	7.7
	As received	4.21	5,200	5,600	4.1	4.0
		4.22	5,050	5,200	5.5	5.0

TABLE 8

TENSILE RESULTS FROM MATERIAL B 2.5

Irradiation Temp. (°C)	Condition	Spec. No.	0.1% Proof Stress (p.s.i.)	U.T.S. (p.s.i.)	% Elong.	% R of A
450	Irradiated	5.1	15,900	17,500	8.0	14
		5.2	17,500	19,200	4.4	7.6
	Heat treated	5.7	10,300	12,300	26.5	30
		5.8	12,600	14,400	34	39
	As received	5.5	12,150	14,500	27	26
		5.6	12,750	15,200	22	27
550	Irradiated	5.9	12,100	12,600	1.4	1.1
		5.10	11,600	12,100	1.3	1.4
	Heat treated	5.15	6,300	7,100	18	18
		5.16	6,600	7,400	22	20
	As received	5.13	8,600	10,100	12	9.4
		5.14	8,900	10,300	11.5	13
650	Irradiated	5.17	–	2,700	0.7	4.3
		5.18	2,600	2,800	0.4	1.6
	Heat treated	5.23	3,200	4,000	12	8.6
		5.24	4,400	5,200	15	6.8
	As received	5.21	4,300	4,700	7.1	7.1
		5.22	4,000	4,600	7.0	6.8

TABLE 9

TENSILE RESULTS FROM MATERIAL B 2.6

Irradiation Temp. (°C)	Condition	Spec. No.	0.1% Proof Stress (p.s.i.)	U.T.S. (p.s.i.)	% Elong.	% R of A
450	Irradiated	6.13	29,000	29,800	20	33
	Heat treated	6.16	23,000	26,900	27	50
	As received	6.15	22,600	30,100	25	42
		6.25	25,400	33,600	19	27
550	Irradiated	6.17	19,100	20,600	8.3	7.4
	Heat treated	6.20	13,600	15,100	21	28
	As received	6.19	13,400	17,700	20.5	19.5
		6.26	14,900	18,600	23	18
650	Irradiated	6.21	7,400	7,700	3.1	0.9
	Heat treated	6.24	4,700	5,600	26.5	12
	As received	6.23	4,800	5,200	20	17
		6.27	3,700	4,600	18	16

TABLE 10

RESULTS OF ELECTRON MICROSCOPY EXAMINATION

Material	Spec. No.	Irrad. Temp. (°C)	% Cleavage Fracture	Intergranular Surfaces	Void Distribution			
					I. G. Void Size		Cleavage Surfaces	Inclusions and Precipitates
					Mean (μ)	Max (μ)		
B 2.2	2.9	550	60	Bubbles on most boundaries. Slightly larger on grain corners.	0.01–0.02	0.03	Small bubbles ($\approx 0.02\,\mu$) occasionally seen within grains.	
	2.17	650	50 – 60	Bubbles on most grain surfaces. Little variation in size or density.	0.03–0.05	0.1	Bubbles (0.02–0.05 μ) on many cleavage surfaces. Density much less than on inter-granular surfaces.	
B 2.3	3.9	550	70 – 80	Most grain surfaces have many bubbles.	0.02–0.04	0.08	Occasional bubbles in grains 0.01 – 0.03 μ	Rounded inclusions on many grain surfaces. Typically 0.5μ dia.
	3.17	650	40 – 50	Many bubbles on grain surfaces, considerable increase in size compared to 550°C irradiation. Occasional large voids (1–2μ) on some boundaries. They have well developed negative crystal shape.	0.05–0.01	0.25	A few bubbles in grains 0.05–0.1μ	
B 2.4	4.9	550	15 – 20	Many bubbles on grain boundaries. Fairly uniform in size and distribution.	0.02 – 0.07	0.16	Bubbles rarely observed.	Many rounded or plate–like inclusions (on boundaries). Identified by selected area diffraction as BeO.
	4.17	650	20	Coarse bubbles on almost all intergranular surfaces. Large size range.	0.05 –0.15	0.7	More frequent than in sample 4.9. Usually 0.01–0.03μ dia. Less cleavage bubbles than in materials B 2.2 and B 2.3.	Many BeO inclusions on grain boundaries.
B 2.5	5.17	650	30	Coarse bubbles on all inter–granular surfaces.	0.05–0.2	0.5	Some bubbles observed 0.03–0.05μ.	Inclusions common on grain boundaries. Usually rounded hexagonal platelets.

TABLE 11

COMPARISON OF MEASURED AND CALCULATED QUANTITIES OF HELIUM

Carrier	Spec. No.	Measured Helium Content (cm^3/cm^3)	Calculated Helium Content (cm^3/cm^3)
B	1.2	0.87	0.84
	1.3	0.93	
D	1.26	0.97	1.08
	1.27	1.10	
F	1.14	0.84	1.00
	1.15	0.79	

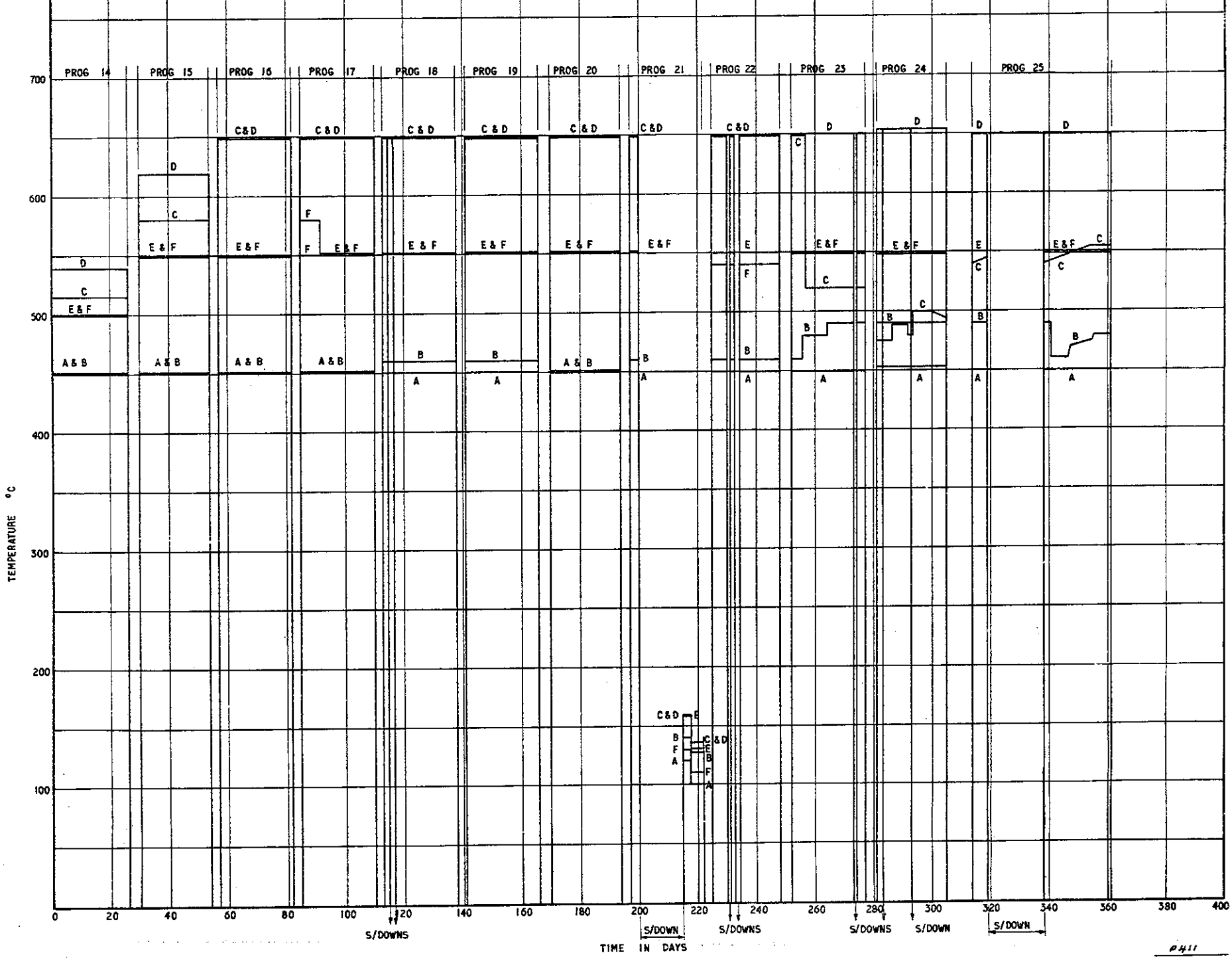

FIGURE 1 X-74 IN-PILE TEMPERATURE CHART

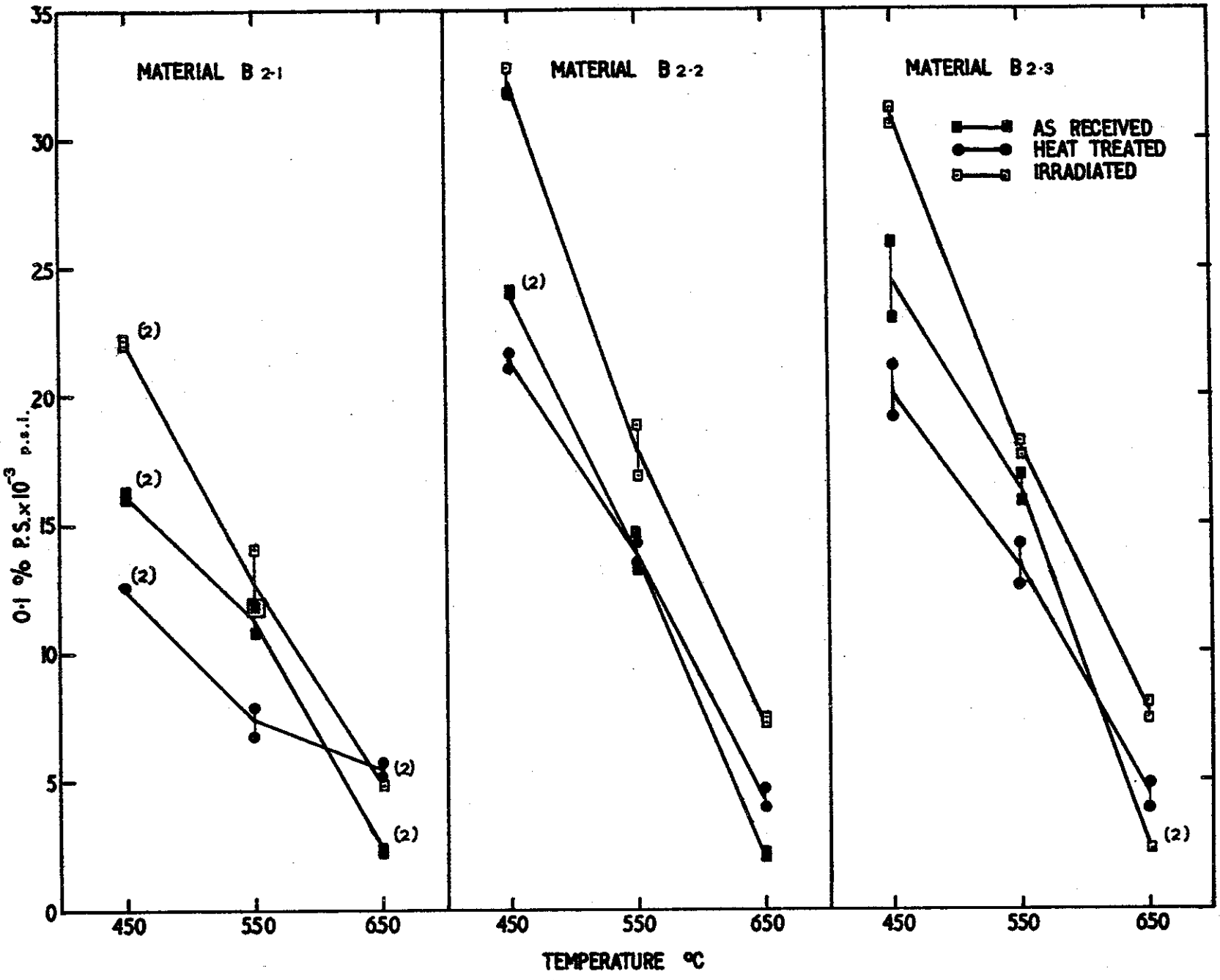

FIGURE 2 PROOF STRESS OF MATERIALS B 2.1, B 2.2, AND B 2.3

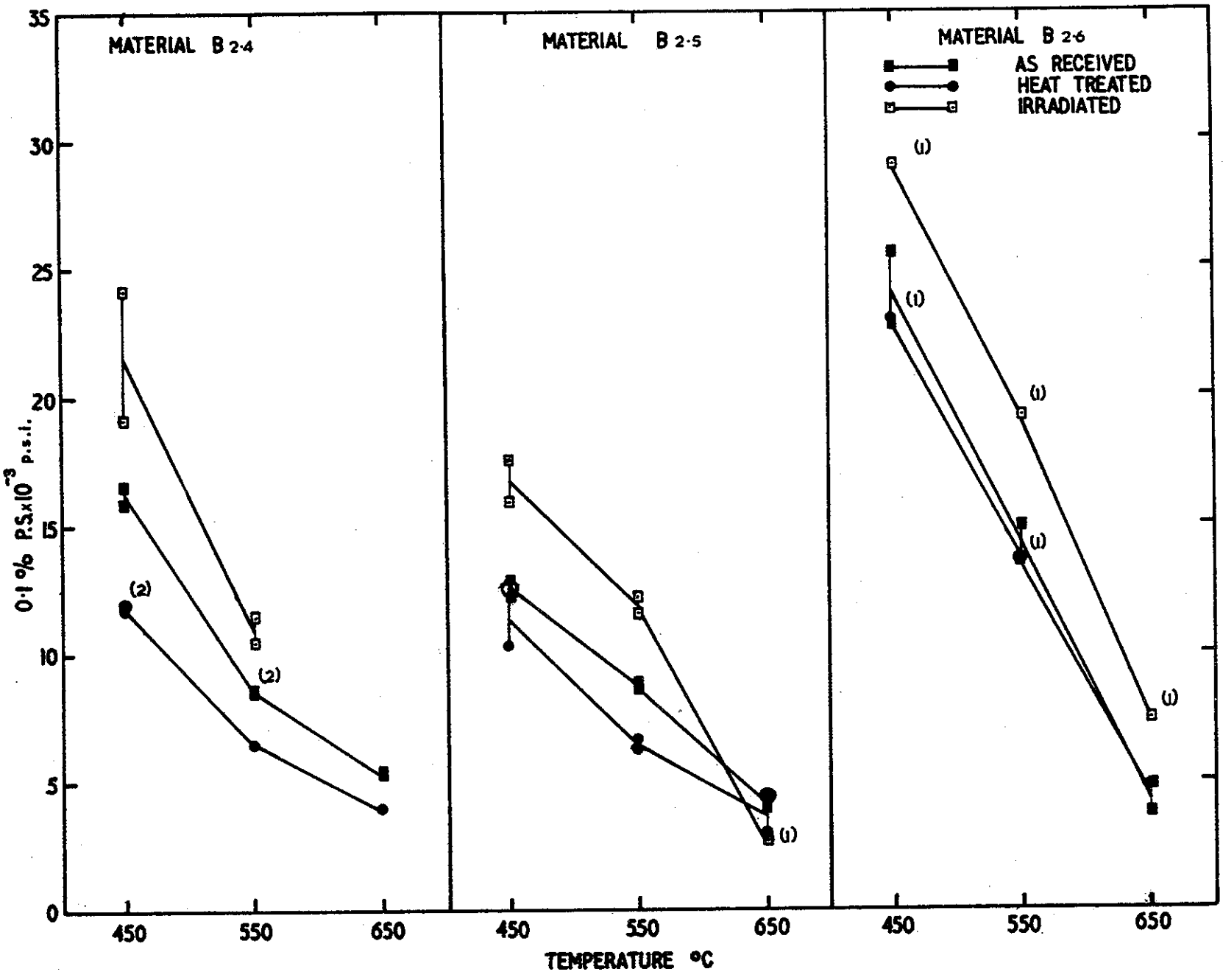

FIGURE 3 PROOF STRESS OF MATERIALS B 2.4, B 2.5, AND B 2.6

P 397

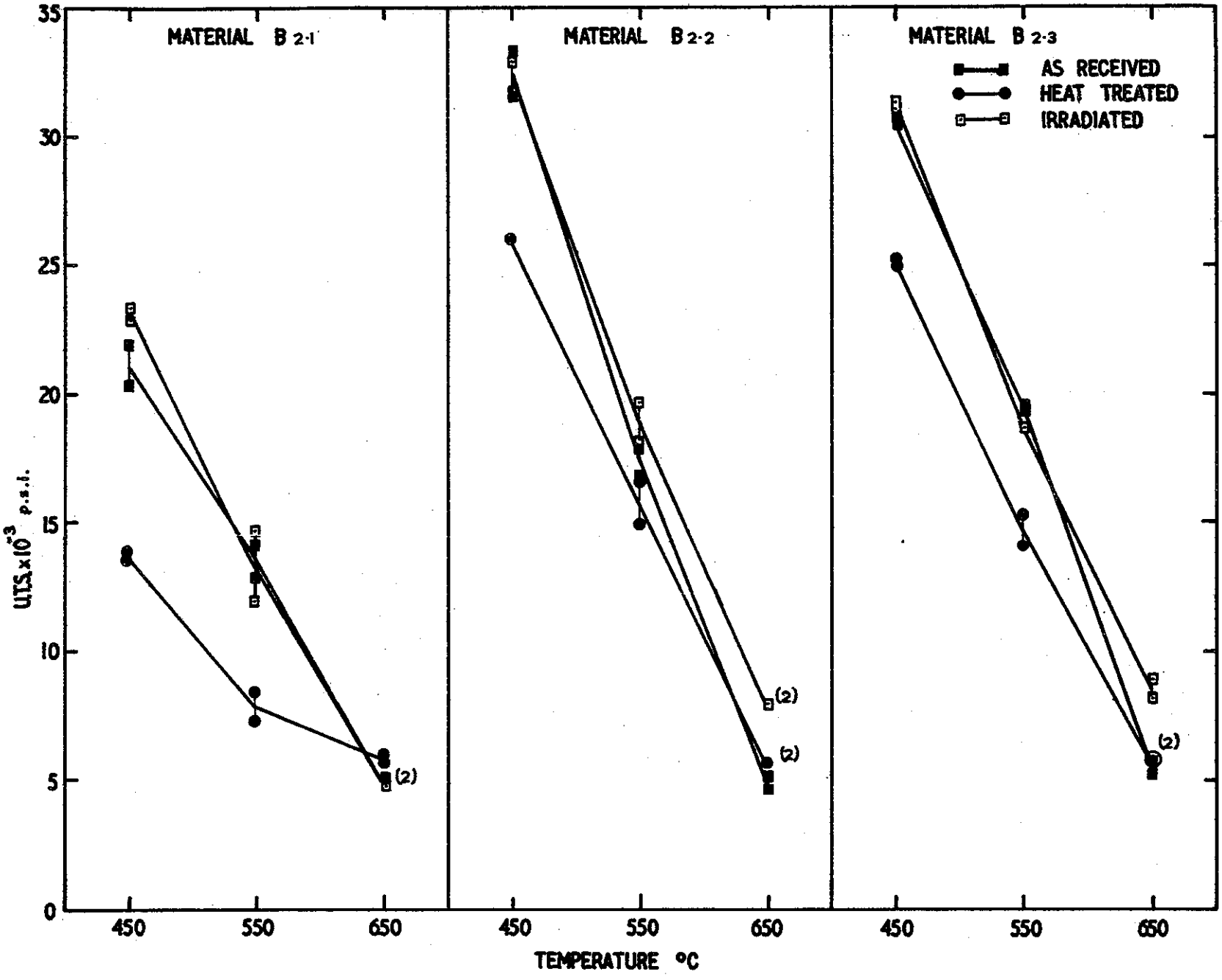

FIGURE 4 U.T.S. OF MATERIALS B 2.1, B 2.2, AND B 2.3

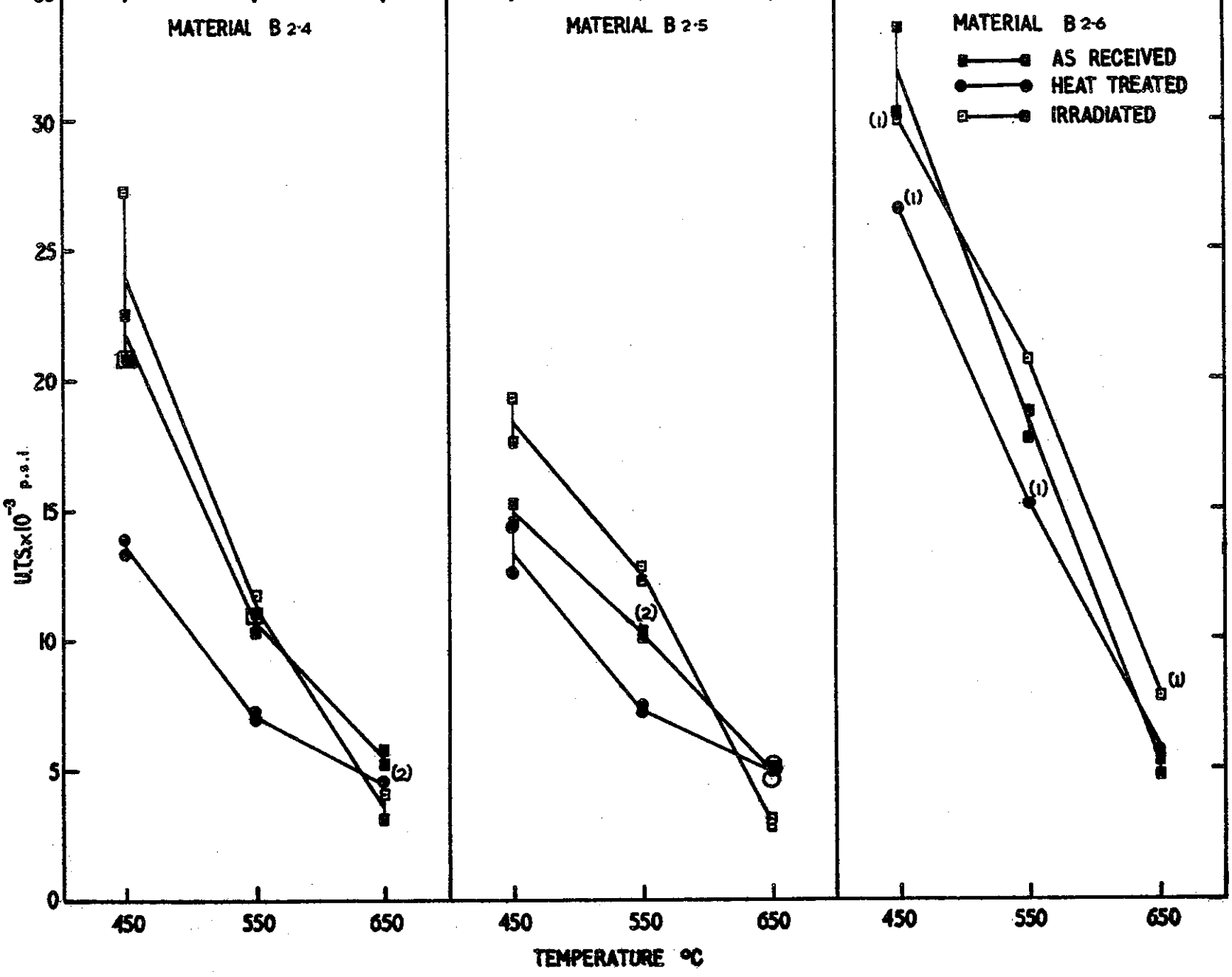

FIGURE 5 U.T.S. OF MATERIALS B 2.4, B 2.5, AND B 2.6

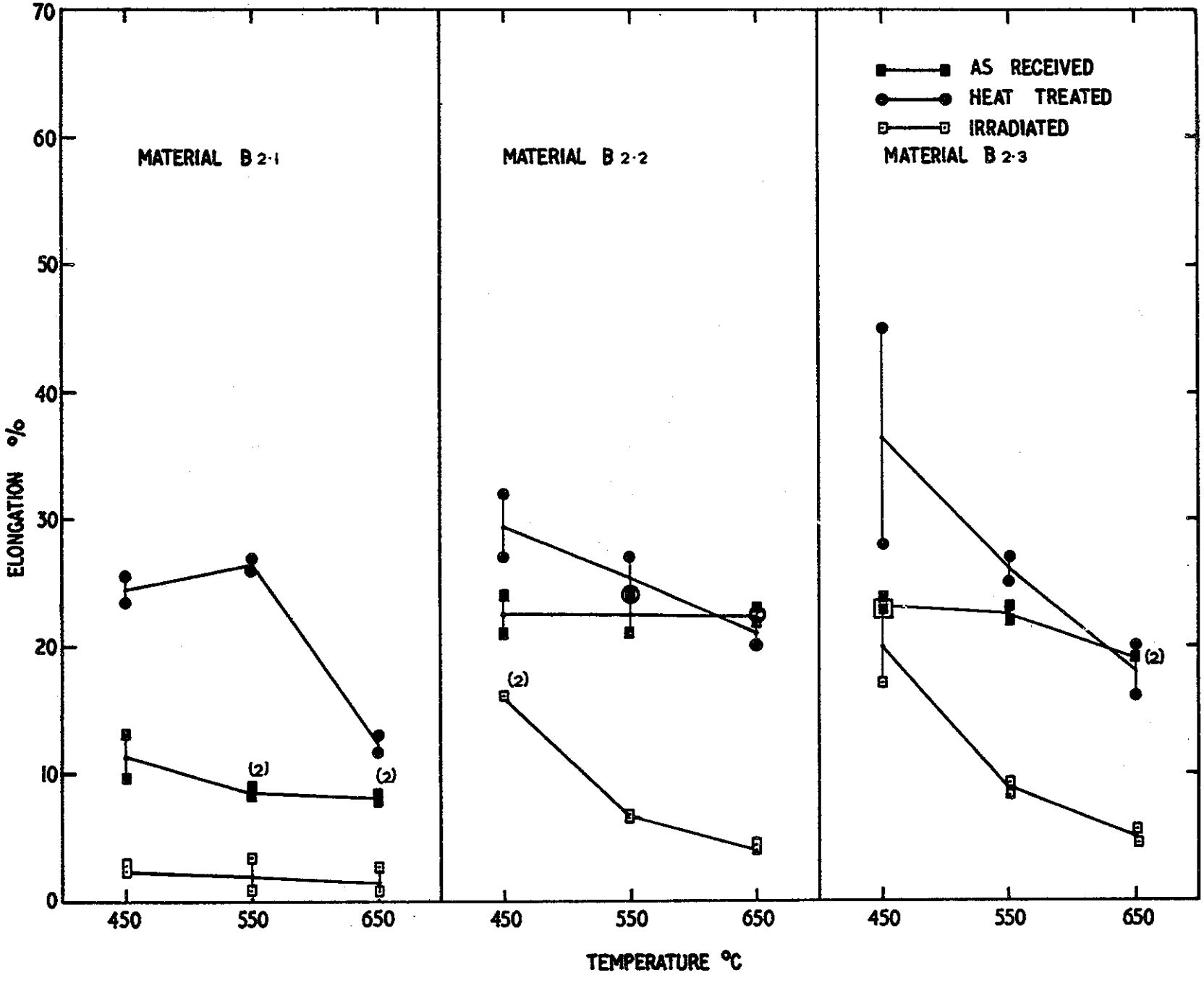

FIGURE 6 ELONGATION OF MATERIALS B 2.1, B 2.2, AND B 2.3

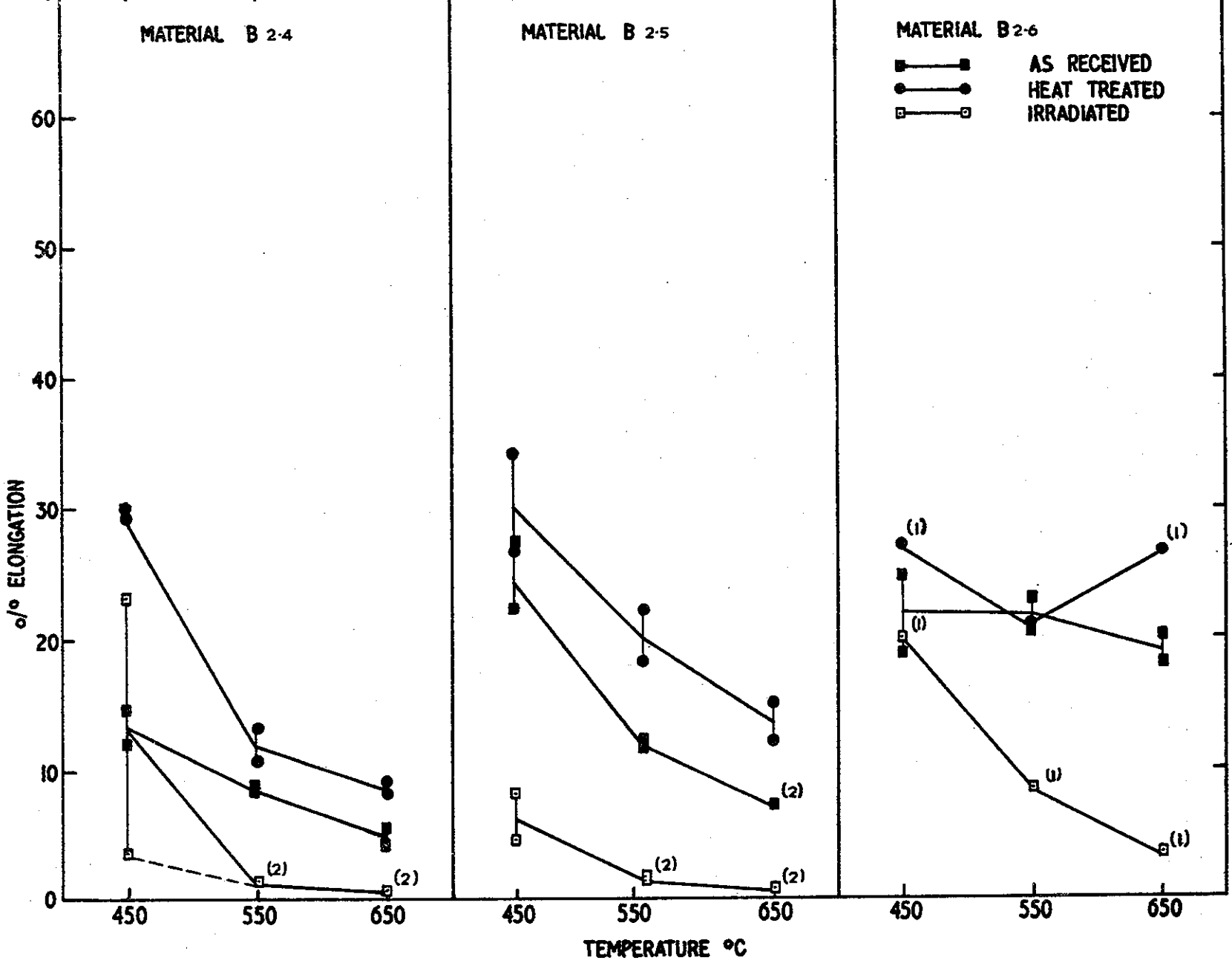

FIGURE 7 ELONGATION OF MATERIALS B 2.4, B 2.5, AND B 2.6

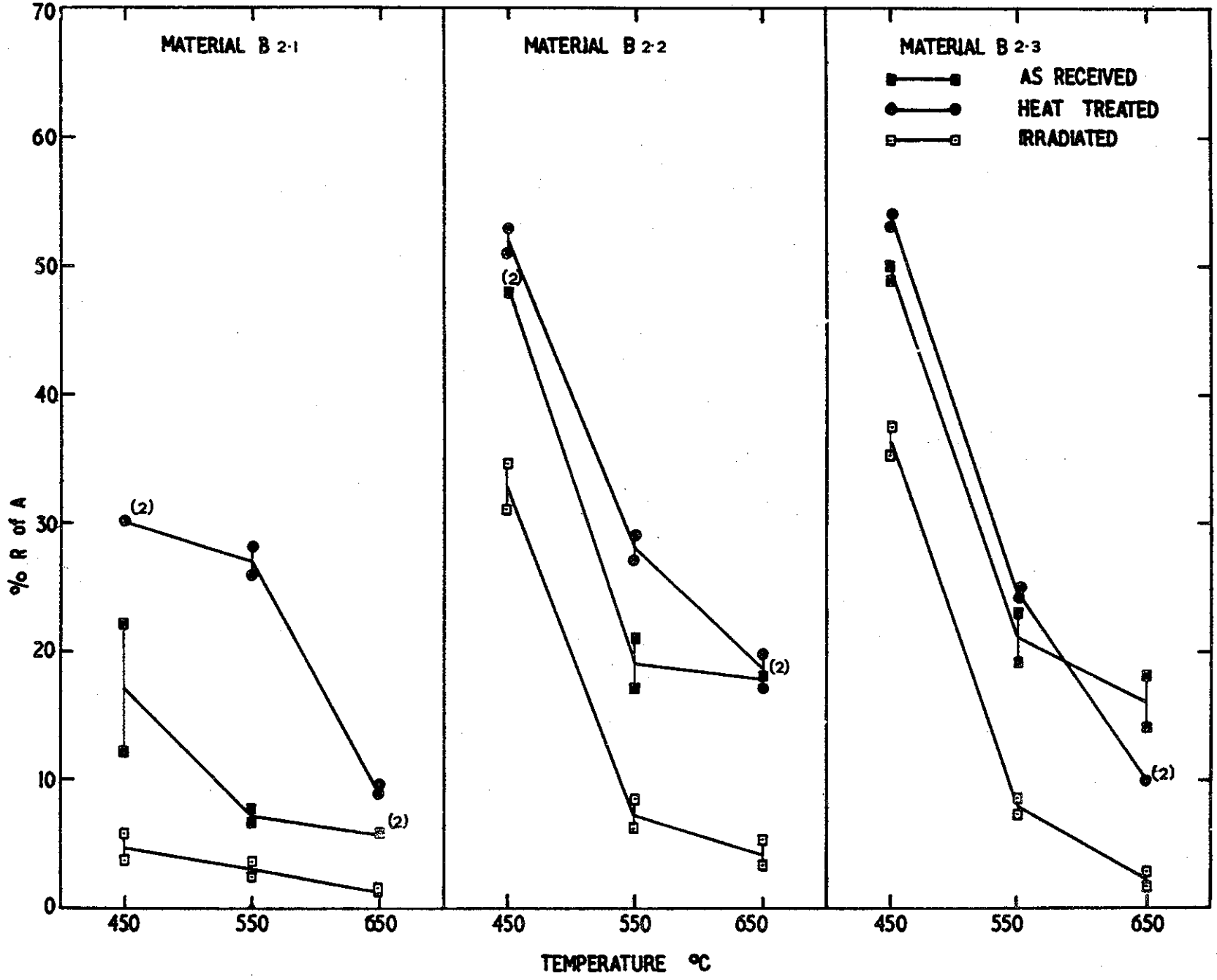

FIGURE 8 REDUCTION IN AREA OF MATERIALS B 2.1, B 2.2, AND B 2.3

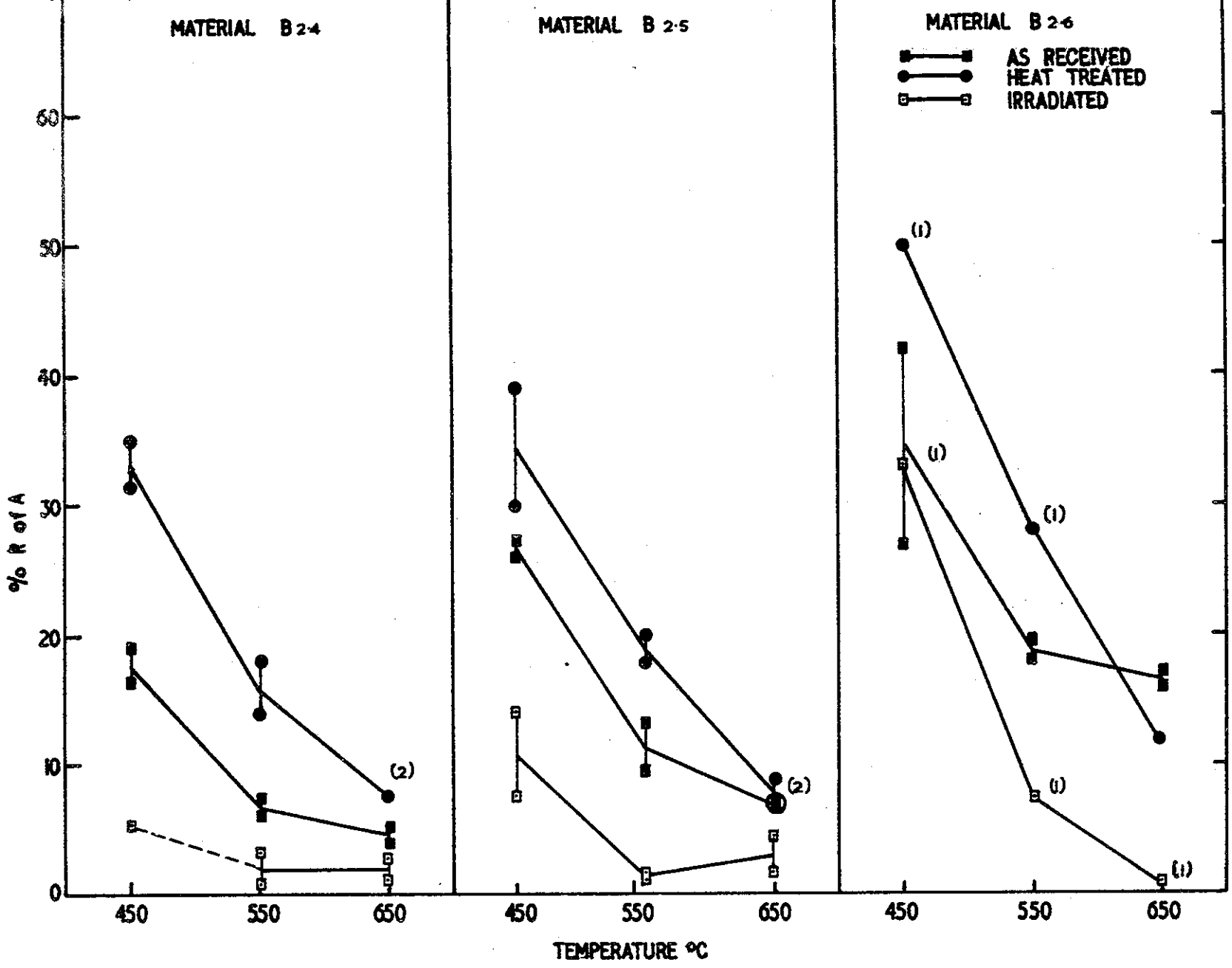

FIGURE 9 REDUCTION IN AREA OF MATERIALS B 2.4, B 2.5, AND B 2.6

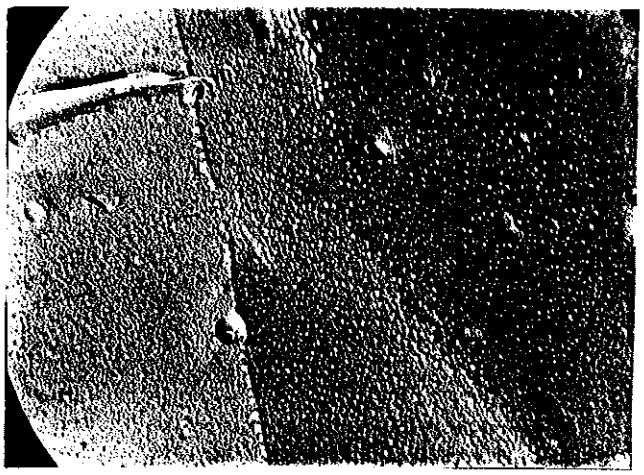

X15,000

(a) Material B2.2

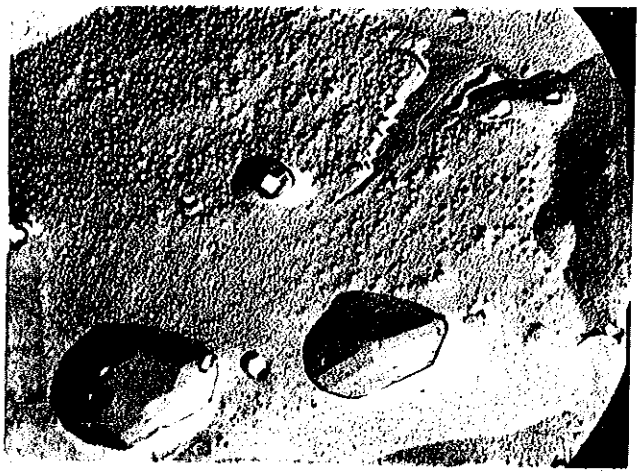

X10,000

(b) Material B2.3

FIGURE 10 ELECTRON-MICROGRAPH OF REPLICAS TAKEN FROM SAMPLES OF HOT PRESSED AND EXTRUDED MATERIALS IRRADIATED AT 650°C

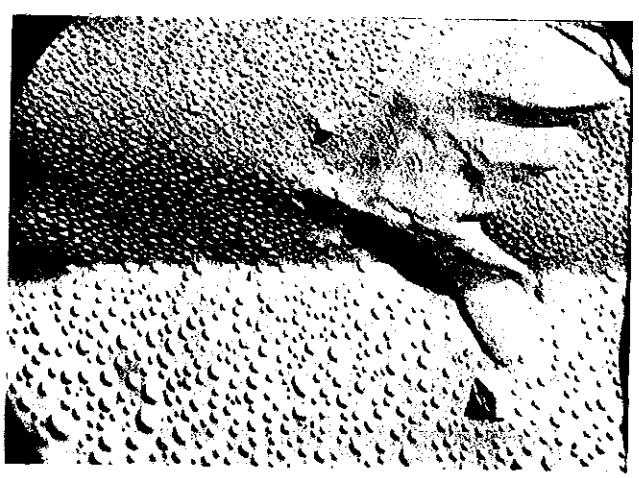

X15,000

(a) Material B2.4

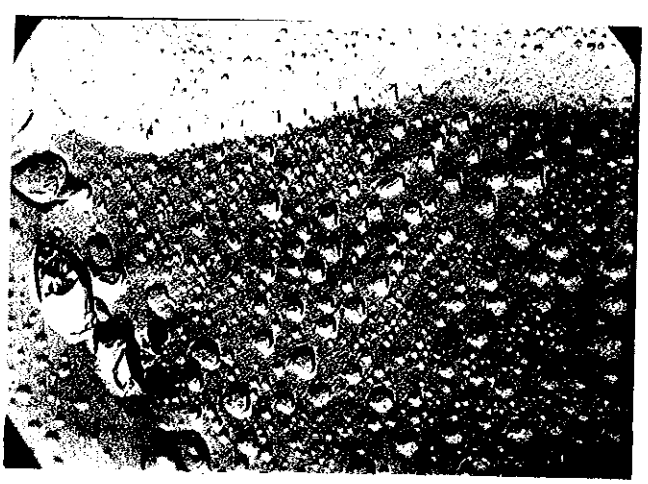

X15,000

(b) Material B2.5

FIGURE 11 ELECTRON-MICROGRAPH OF REPLICAS TAKEN FROM SAMPLES OF LOOSE SINTERED AND EXTRUDED MATERIALS IRRADIATED AT 650°C